BNL-220641-2020-TECH
C-A/AP/636

Effects of coherent offset of velocity distribution in electron coolers on ion dynamics

S. Seletskiy

November 2020

Collider Accelerator Department
Brookhaven National Laboratory

U.S. Department of Energy
USDOE Office of Science (SC), Nuclear Physics (NP) (SC-26)

DISCLAIMER

Effects of coherent offset of velocity distribution in electron coolers on ion dynamics

S. Seletskiy*, A. Fedotov

November 16, 2020

Abstract

We revisit the effect of coherent offset in velocity distribution of the electron beam in electron coolers and consider its implications for the dynamics of the cooled ion bunch. This effect becomes of special importance for high-energy electron coolers due to reduction of transverse angular spread with energy, thus requiring strict control. As an example, estimates of the severity of and the possibility to observe the considered effects for LEReC case are discussed.

1 Introduction

In electron cooling [1, 2] a "cold" electron beam co-traveling with the ion beam in a common section of the storage ring, called cooling section (CS), introduces a dynamical friction [3] to the ions. The dynamical friction force reduces both the angular and the energy spread of the ion bunch, thus cooling it.

Nonetheless, if the velocity distribution of the electron bunch has a coherent offset with respect to the average velocity of the affected ion bunch then, under specific conditions, the ion bunch can exhibit unusual behavior. Such as, bifurcations of bunch density and formation of two-hump density distribution. These effects can also lead to a decrease in a lifetime of the ion bunch.

*seletskiy@bnl.gov

Thorough theoretical studies of the coherent offset effects were performed by Ya. Derbenev [4]. Experimental observations of resulting ion beam dynamics can be found, for instance, in [5, 6].

In this paper we will review the theory of electron cooling with coherent velocity offset. Next, we will explore the effect of coherent excitation using a simple simulation model. Finally, we will apply the derived formulas to electron-ion beam dynamics in LEReC.

2 Cooling force formulas for electron beam distribution with coherent offset

The friction force acting on an ion co-traveling with an electron bunch with velocity distribution $f(v_e)$ is given by [7, 8]:

$$\vec{F} = -\frac{4\pi n_e e^4 Z^2}{m_e} \int L_C \frac{\vec{v} - \vec{v}_e}{|\vec{v} - \vec{v}_e|^3} f(v_e) d^3 v_e \tag{1}$$

Here, n_e is the electron bunch density in the beam frame, e is the electron charge, $Z \cdot e$ is the ion charge, m_e is the mass of the electron, $\vec{v}$ and $\vec{v}_e$ are ion and electron velocities in the beam frame and L_C is the Coulomb logarithm, which can be assumed to be constant, in the LEReC case $L_C \approx 8$, for example.

If we assume a Gaussian distribution of velocities in the electron bunch then Eq. (1) can be simplified to 1D integrals for each component of the friction force [9]. Of course, such formulas (named Binney's formulas) are much more convenient for numerical simulations and are what we need for the studies described in this paper.

It is worth pointing out, that for the case of isotropic velocity distribution ($\Delta_x = \Delta_y = \Delta_z \equiv \Delta$), the integrals in Binney's formulas can be taken analytically, as will be shown below. For the physics of the effects which we are considering in this paper there is no qualitative difference between isotropic and anisotropic distributions in e-bunch velocities. Yet, it is very important for quantitative estimates to have proper expressions for a more general anisotropic case.

We will derive Binney's formulas for v-distribution with coherent offset by following a detailed example [10] of derivation of Binney's formulas for electron coolers for no-offset v-distribution.

The electron bunch v-distribution is given by:

$$f(v_e) = \frac{1}{(2\pi)^{3/2}\Delta_x\Delta_y\Delta_z} \exp - \left(\frac{(v_{ex}-\mu_x)^2}{2\Delta_x^2} + \frac{(v_{ey}-\mu_y)^2}{2\Delta_y^2} + \frac{(v_{ez}-\mu_z)^2}{2\Delta_z^2} \right) \tag{2}$$

Let us introduce an effective potential in a velocity-space:

$$U = C_0 \int \frac{f(v_e)}{|\vec{v}-\vec{v_e}|} d^3 v_e \tag{3}$$

such that

$$F_{x,y,z} = \partial U / \partial v_{x,y,z} \tag{4}$$

Here, $C_0 = \frac{4\pi n_e e^4 Z^2 L_C}{m_e}$.

Noticing that $1/|\vec{v}-\vec{v_e}|$ can be represented as:

$$\begin{aligned} &\frac{1}{\sqrt{(v_x-v_{ex})^2+(v_y-v_{ey})^2+(v_z-v_{ez})^2}} = \\ &\frac{2}{\sqrt{\pi}} \int_0^\infty \exp\left[-p^2\left((v_x-v_{ex})^2+(v_y-v_{ey})^2+(v_z-v_{ez})^2\right)\right] dp \end{aligned} \tag{5}$$

we get from Eqs. (2)-(5):

$$\begin{aligned} U = &\frac{C_0}{\sqrt{2}\pi^2\Delta_x\Delta_y\Delta_z} \int_0^\infty \left[\int_{-\infty}^\infty e^{-p^2(v_x-v_{ex})^2 - \frac{(v_{ex}-\mu_x)^2}{2\Delta_x^2}} dv_{ex} \right. \\ &\left. \int_{-\infty}^\infty e^{-p^2(v_y-v_{ey})^2 - \frac{(v_{ey}-\mu_y)^2}{2\Delta_y^2}} dv_{ey} \int_{-\infty}^\infty e^{-p^2(v_z-v_{ez})^2 - \frac{(v_{ez}-\mu_z)^2}{2\Delta_z^2}} dv_{ez} \right] dp \end{aligned} \tag{6}$$

Since:

$$\int_{-\infty}^\infty e^{-p^2(v_x-v_{ex})^2 - \frac{(v_{ex}-\mu_x)^2}{2\Delta_x^2}} dv_{ex} = \sqrt{2\pi}\Delta_x \frac{\exp\left(-\frac{p^2(v_x-\mu_x)^2}{1+2p^2\Delta_x^2}\right)}{\sqrt{1+2p^2\Delta_x^2}} \tag{7}$$

we get for the effective potential:

$$U = \frac{2C_0}{\sqrt{\pi}} \int_0^\infty \frac{\exp\left(-\frac{p^2(v_x-\mu_x)^2}{1+2p^2\Delta_x^2} - \frac{p^2(v_y-\mu_y)^2}{1+2p^2\Delta_y^2} - \frac{p^2(v_z-\mu_z)^2}{1+2p^2\Delta_z^2}\right)}{\sqrt{(1+2p^2\Delta_x^2)(1+2p^2\Delta_y^2)(1+2p^2\Delta_z^2)}} dp \tag{8}$$

From Eqs. (4) and (8) we obtain Binney's formulas. For example, for F_x:

$$F_x = -\frac{4C_0}{\sqrt{\pi}} \int_0^\infty \frac{p^2(v_x-\mu_x)}{1+2p^2\Delta_x^2} \frac{\exp\left(-\frac{p^2(v_x-\mu_x)^2}{1+2p^2\Delta_x^2} - \frac{p^2(v_y-\mu_y)^2}{1+2p^2\Delta_y^2} - \frac{p^2(v_z-\mu_z)^2}{1+2p^2\Delta_z^2}\right)}{\sqrt{(1+2p^2\Delta_x^2)(1+2p^2\Delta_y^2)(1+2p^2\Delta_z^2)}} dp \tag{9}$$

A more conventional and maybe more elegant form of Binney's formulas is obtained by substituting $p^2 = 1/(2q\Delta_t^2)$ into expressions (9), here we are assuming $\Delta_x = \Delta_y \equiv \Delta_t$. Then we get:

$$\left\{ \begin{array}{rcl} F_{x,y} & = & -C(v_{x,y}-\mu_{x,y}) \int_0^\infty g_t(q)dq \\ F_z & = & -C(v_z-\mu_z) \int_0^\infty g_z(q)dq \\ g_t(q) & = & \frac{1}{\Delta_t^2(1+q)^2\sqrt{\Delta_t^2 q+\Delta_z^2}} \exp\left[-\frac{(v_x-\mu_x)^2+(v_y-\mu_y)^2}{2\Delta_t^2(1+q)} - \frac{(v_z-\mu_z)^2}{2(\Delta_t^2 q+\Delta_z^2)}\right] \\ g_z(q) & = & \frac{1}{(1+q)(\Delta_t^2 q+\Delta_z^2)^{3/2}} \exp\left[-\frac{(v_x-\mu_x)^2+(v_y-\mu_y)^2}{2\Delta_t^2(1+q)} - \frac{(v_z-\mu_z)^2}{2(\Delta_t^2 q+\Delta_z^2)}\right] \end{array} \right. \tag{10}$$

where $C = 2\sqrt{2\pi} n_e r_e^2 m_e c^4 Z^2 L_C$.

In case of $\mu_{x,y,z} = 0$ one can introduce $v_t = \sqrt{v_x^2+v_y^2}$ and $F_t = \sqrt{F_x^2+F_y^2}$ and Binney's formulas (10) take a form as implemented in the BETACOOL code [11].

In case of isotropic velocity distribution Eq. 10 results in a simple analytic formula:

$$\left\{ \begin{array}{rcl} F_{x,y,z} & = & -\frac{C}{\Delta^3 a^3}(v_{x,y,z}-\mu_{x,y,z}) \left[-2ae^{-a^2/2} + \sqrt{2\pi}\mathrm{Erf}\left(\frac{a}{\sqrt{2}}\right)\right] \\ a & = & \sqrt{(v_x-\mu_x)^2+(v_y-\mu_y)^2+(v_z-\mu_z)^2}/\Delta \end{array} \right. \tag{11}$$

Here the error function Erf(z) $\equiv \frac{2}{\sqrt{\pi}} \int_0^z e^{-t^2} dt$.

Formulas (10) present the dependence of the components of the dynamical friction force on the ion's velocity in a form convenient for numerical integration. Figure 1 shows the results of such calculations for the operational LEReC parameters. As one can see, the presence of a coherent offset in the velocity distribution of the electron bunch manifests itself in a respective shift of the force function w.r.t. the zero ion velocity.

3 Dynamics of the ion experiencing cooling force with coherent offset

The turn-by-turn dynamics of the uncoupled transverse motion of the ion, in the presence of external friction force due to the electrons, can be represented

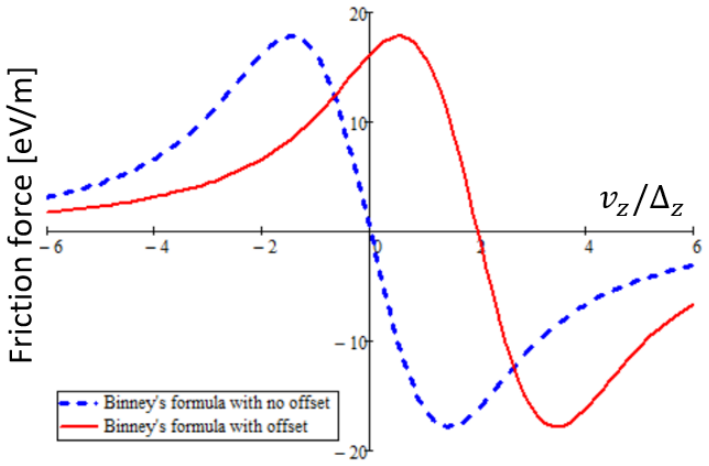

Figure 1: Longitudinal component of the friction force for the v-distribution of the electron bunch having a coherent offset $\mu_z = 2\Delta_z$ (solid red line) and for the v-distribution with no offset (dashed blue line).

in Courant-Snyder coordinates ($\xi = x/\sqrt{\beta_T}$, $\zeta = \alpha_T x/\sqrt{\beta_T} + \sqrt{\beta_T}x'$, where α_T and β_T are Twiss parameters) as:

$$\xi'' + (2\pi)^2\xi = 2\pi\frac{\sqrt{\beta_{CS}}F_x L_{CS}}{m_i c^2\beta^2}\mathrm{comb}(1+\nu_x) \tag{12}$$

Here m_i is the mass of an ion, β_{CS} is β_T in the cooling section, to reduce the simulations time and without a loss of generality we substitute a tune Q_x with $1+\nu_x$, where ν_x is a fractional horizontal tune, and we define the comb function as:

$$\mathrm{comb}(1+\nu_x) = \begin{cases} 1 & , \quad \mathfrak{s} = n(1+\nu_x) \\ 0 & , \quad \mathfrak{s} \neq n(1+\nu_x) \end{cases} \tag{13}$$

where an independent variable $\mathfrak{s}$ in Eqs. 12 and 13 is a fraction of a betatron oscillation and integer $n = 1, 2 \ldots \infty$.

Equation of motion (12) can be integrated numerically. Yet, prior to simulating the dynamics of the ion bunch let us consider the physics of an ion interaction with the offset cooling force.

3.1 Qualitative analysis of ion-electron interaction

As one can easily see from Fig. 1, the electron bunch with the coherent offset in its v-distribution creates a friction force that causes an excitation rather

than a damping of the ion's oscillations for ions with $v \in [0, \mu]$. Let us denote the friction force in this velocity range as F_+.

The ion having the velocity $v \in [-\mu, \mu]$ will experience the exciting friction force F_+ on some turns in the storage ring and the damping friction force F_- on the other turns depending on its betatron phase. Whether the average friction force experienced by the ion is damping or exciting the betatron oscillations depends on the relation between F_+ and F_-.

Let us consider two scenarios.

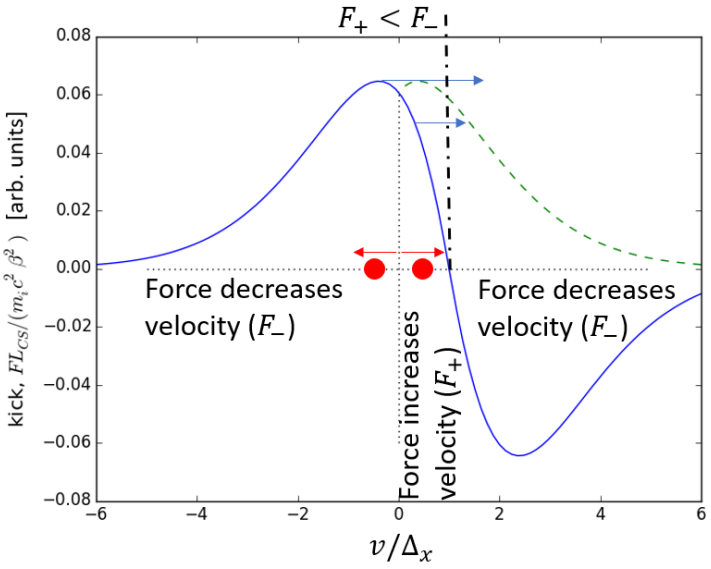

Figure 2: The friction force produced by e-bunch with v-distribution with a "small" coherent velocity shift (blue solid line). The green dashed line is a reflection of the friction force acting on the ions with $v < 0$ across the vertical axis, and is shown to make the visual comparison of F_+ and F_- easier.

Under the first scenario, demonstrated in Fig. 2, the coherent shift μ is smaller than the velocity at which the first derivative of the friction force changes sign ($v \approx \Delta_x$). For that case $F_+ < F_- \ \forall v \in [-\infty, \infty]$, therefore the ions at all betatron amplitudes will experience the net cooling force.

Under the second scenario (Fig. 3) the coherent shift μ is larger than the velocity at which the first derivative of the friction force changes sign. For that case, the net friction force acting on ions with small betatron amplitudes excites the betatron oscillations. Indeed, as Fig. 3 demonstrates, $F_+ > F_- \ \forall v \in [-\mu, \mu]$ and the net friction force is an exciting one rather than a damping one. On the other hand, the ions with large betatron amplitudes still experience a net damping force. Hence, all the ions will eventually reach

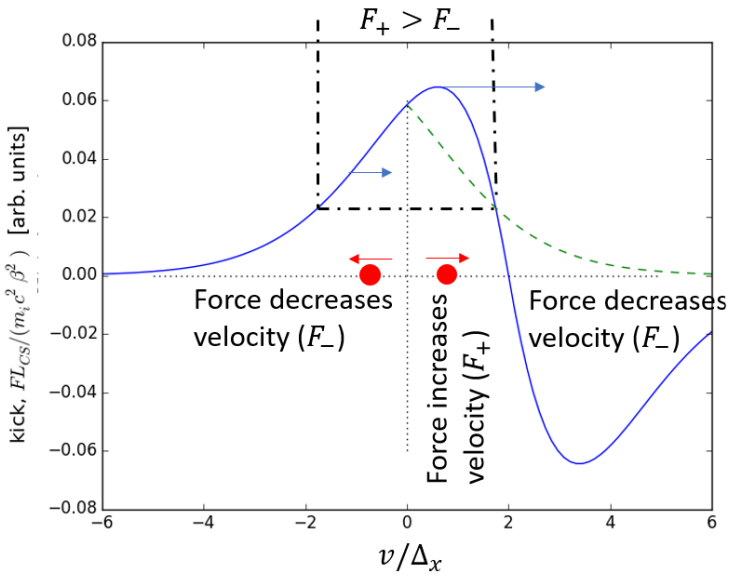

Figure 3: The friction force produced by e-bunch with v-distribution with a "large" coherent velocity shift (blue solid line). The green dashed line is a reflection of the friction force acting on the ions with $v < 0$ across the vertical axis, and is shown to make the visual comparison of F_+ and F_- easier.

the phase space amplitude ($J = \sqrt{\xi^2 + \zeta^2}$), which can be roughly estimated as:

$$J_0 \approx \frac{\sqrt{\beta_{CS}}\mu}{\gamma\beta c} \tag{14}$$

Therefore, for the second case we expect that the shifted friction force will create a circular attractor in the phase space and that with enough time allowed all the ions will be performing the betatron oscillations with J_0, thus forming a ring-shaped distribution in the phase space. The projection of the phase space doughnut on the physical space will be observed as a double-hump density distribution.

It is worth to mention that the formation of the circular attractor in the phase space is possible only because the friction force is non-monotonic. The non-linearity of the friction force alone is not enough to create conditions necessary for this interesting phenomenon.

3.2 Numerical studies of ion bunch dynamics

We assume $\alpha_T = 0$ in the CS (which is a typical setup) and for the sake of convenience we rewrite Eq. (12) as:

$$\chi'' + (2\pi)^2\chi = \frac{L_{CS}F_x(\chi'\sigma_\theta\gamma\beta c)}{\sigma_\theta m_i c^2\beta^2}\mathrm{comb}(1+\nu_x) \tag{15}$$

where we introduced new variable $\chi \equiv x/(2\pi\sigma_\theta\beta_{CS})$ and explicitly wrote $F_x(v_x)$ in terms of χ'.

We integrate Eq. (15) numerically with an explicit, exactly simplectic, third order method [12]. To accelerate the numerical studies we will use a large friction kick (see Fig. 4), so that the effect of excitation is clearly seen after a few hundred turns.

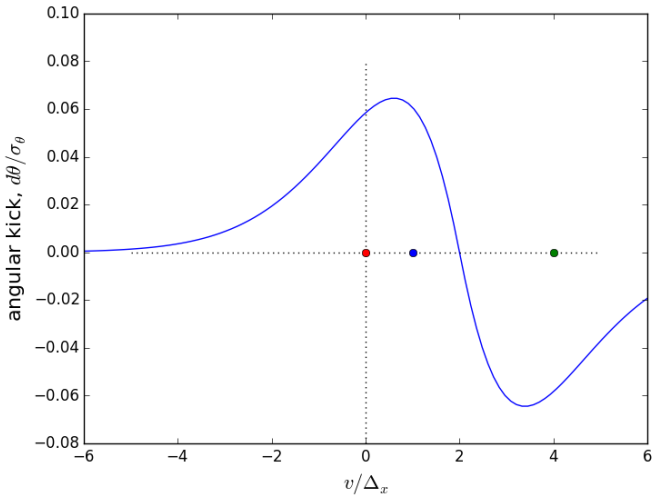

Figure 4: The angular kick produced by friction force (blue line). This kick is used in numerical studies described in Section 3.2. The green, red and blue circles show the initial velocities of the three test particles.

First, we track three sample ions for 500 turns in the presence of friction force produced by electron bunch with v-distribution having a coherent shift $\mu_x = 0.8\Delta_x$. As was expected from considerations in section 3.1 the cooling process goes undisturbed when μ is smaller than the velocity for which the friction force is maximized (Fig. 5).

Second, we track three sample ions for 1000 turns in the presence of friction force produced by electron bunch with v-distribution having a coherent shift $\mu_x = 2\Delta_x$. As one can see from Fig. 6 all three ions reach the circular attractor after several hundred turns.

Next, we study the evolution of the ion bunch in the phase space. We start with the bunch having the Gaussian distribution and observe its behavior in the presence of the circular attractor. Figure 7 shows that in the ideal linear

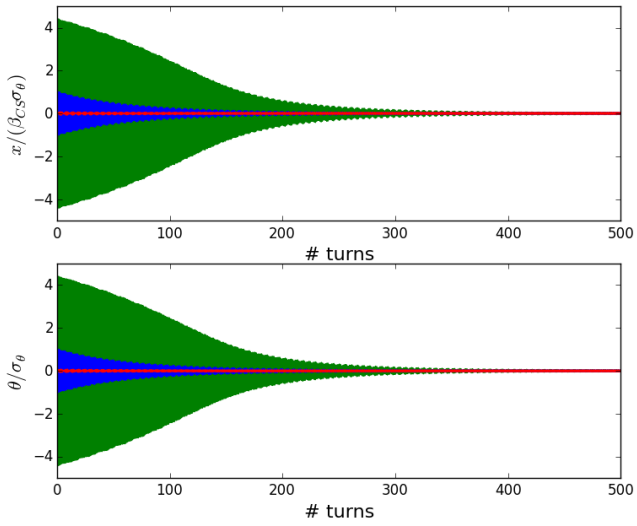

Figure 5: Dynamics of the three test ions cooled by e-beam with $\mu = 0.8\Delta_x$.

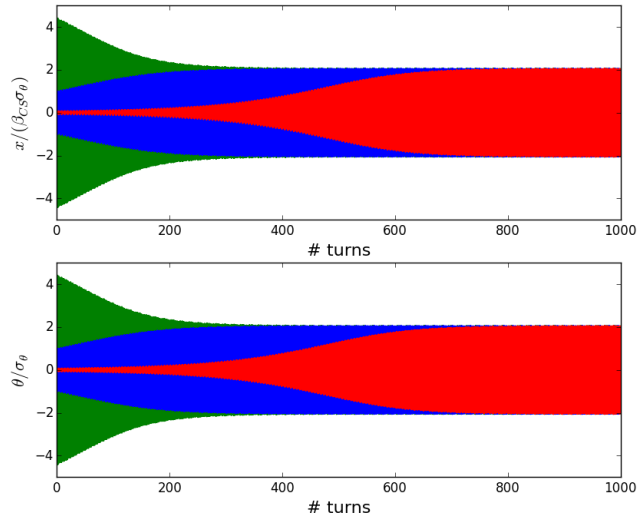

Figure 6: Dynamics of the three test ions in the presence of force shown in Fig 4 ($\mu = 2\Delta_x$).

machine in the absence of any additional effects the phase space ring is well developed after 500 turns. We can make a conclusion that the reasonable measure of a characteristic time of the formation of the phase space ring (τ_R)

is the time that it takes an ion with a zero initial betatron amplitude to reach the circular attractor.

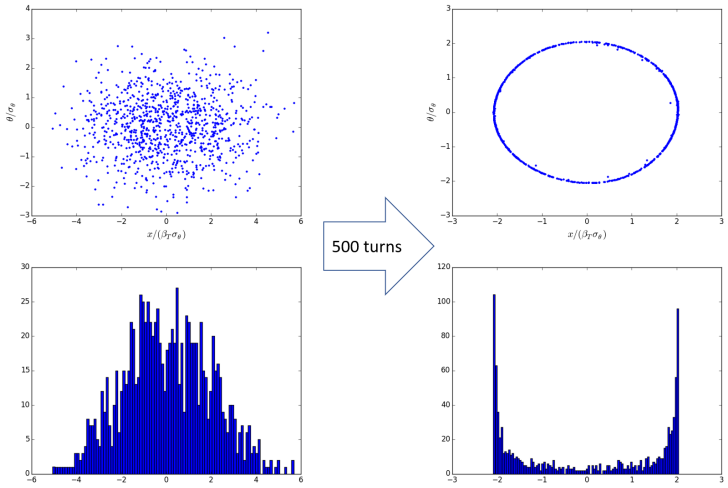

Figure 7: Formation of the circular distribution in the phase space and of the respective two-hump distribution in the physical space in the presence of circular attractor.

Of course, the tune spread erodes the perfect phase space circle turning it into a doughnut (Fig. 8).

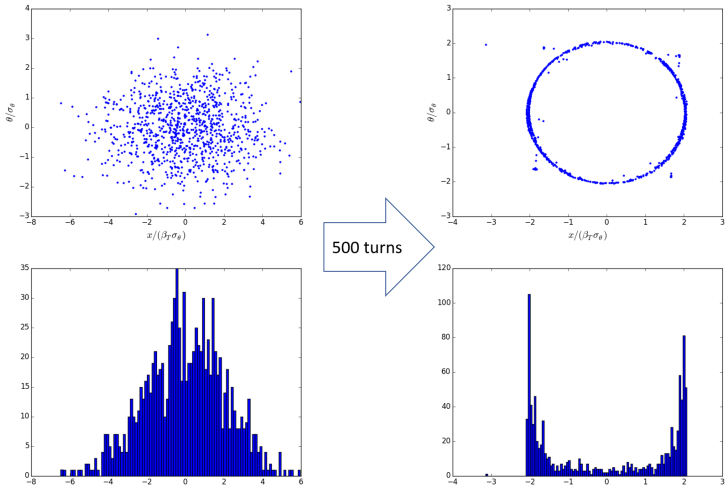

Figure 8: Evolution of the ion bunch with the tune spread with $\sigma_\nu = 0.01\nu_0$ in the presence of circular attractor.

A presence of the IBS, or of any other heating mechanism for that matter, farther dilutes the circular distribution in the phase space. The shape of a

final balanced distribution depends on the relative strength of the cooling (without coherent shift) and heating forces.

For example, Fig. 9 shows the formation of the phase space doughnut when the diffusion is about ten times smaller than the cooling. Figure 10 shows the case of the diffusion being just two times weaker than the cooling. For that case the presence of the circular attractor is completely masked by the IBS heating and qualitatively the effect of the coherent offset in v-distribution becomes indistinguishable from an effect of the increase in the rms spread of v-distribution of the electron bunch.

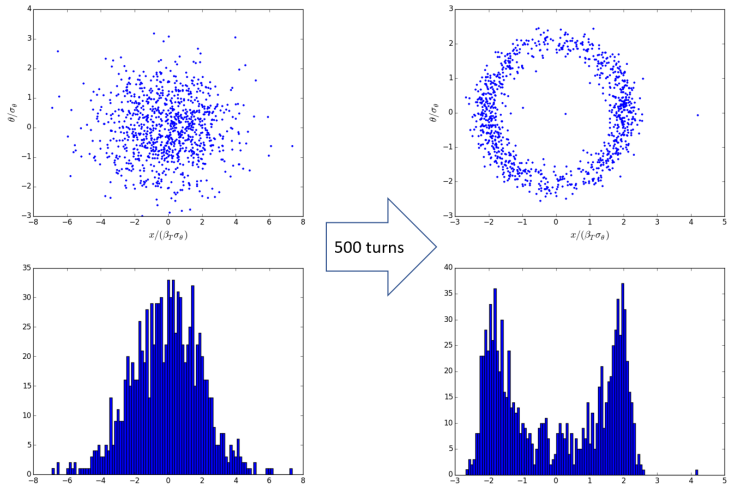

Figure 9: Effect of the circular attractor on the evolution of the ion bunch in the presence of weak IBS (diffusion is about ten times weaker than the cooling without coherent shift in v-distribution).

Finally, if one introduces the coherent shift after the ion bunch is cooled to low emittance then one can observe the bifurcations of the ion bunch density. As Fig. 11 demonstrates, such an effect results from the small emittance i-bunch orbiting along the circular attractor.

All the effects studied in this section are relevant for the longitudinal direction as well as for the transverse one. In the next section we will apply the theory of coherent excitation, which we developed here, to the ion beam dynamics in LEReC.

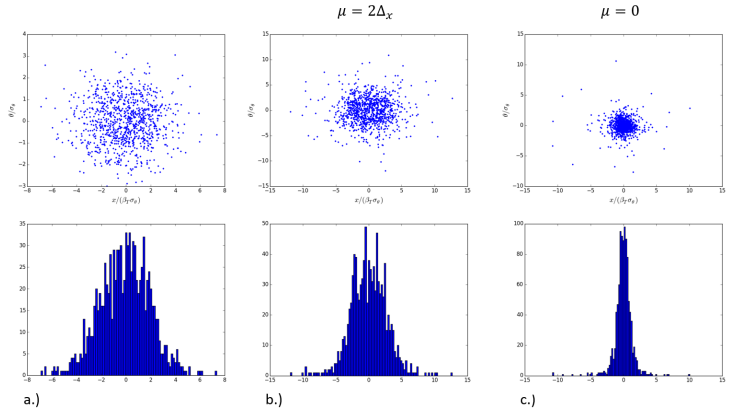

Figure 10: Effect of the circular attractor on the evolution of the ion bunch in the presence of strong IBS (diffusion is about 2 times weaker than the cooling without coherent shift in v-distribution). Plot (a.) shows an initial ion bunch's distribution, plot (b.) shows the balance distribution in the presence of circular attractor, plot (c.) shows the cooling by e-beam with zero offset in v-distribution.

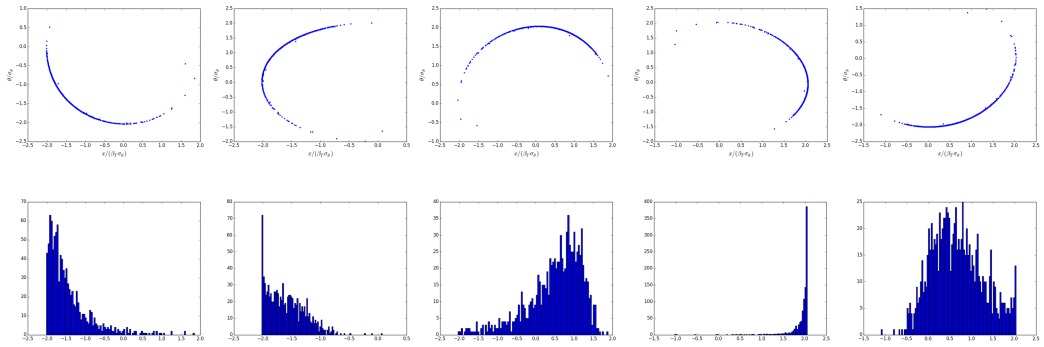

Figure 11: The density distribution of the ion bunch bifurcates as the small-emittance bunch goes along the circular attractor in the phase space.

4 Implications of coherent excitation theory for beam dynamics in LEReC

For operational LEReC parameters the angular kick obtained by an ion interacting with the electron bunch on a single pass through the CS is shown in Fig. 12. The force in Fig. 12 is given for coherent angular misalignment of $\theta = 2\sigma_\theta$ between the electron and the ion trajectories.

To determine the characteristic time of the transverse coherent excitation (τ_{Rt}) in LEReC we numerically solve Eq. (15) for an ion with a zero initial

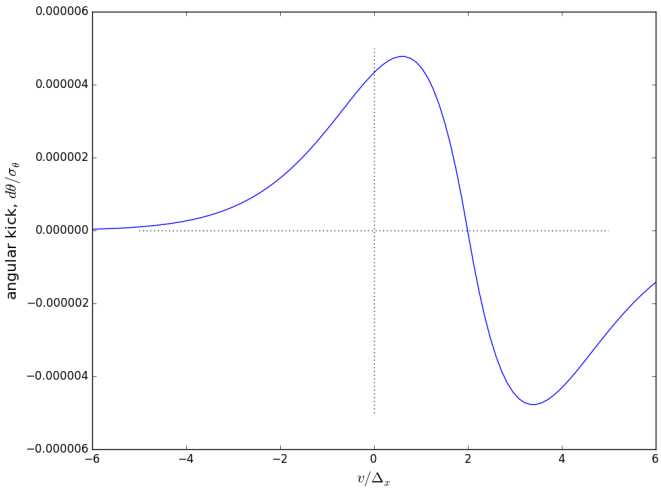

Figure 12: Angular kick for operational LEReC parameters.

betatron amplitude. To reduce the simulation's time we assume that an ion interacts with the electron beam on each turn in RHIC. In reality, due to a picket-fence time structure of the LEReC macro-bunch, the rms ion sees the electron beam on average every fourth turn. Hence, the characteristic time obtained from simulations must be multiplied by a factor of four.

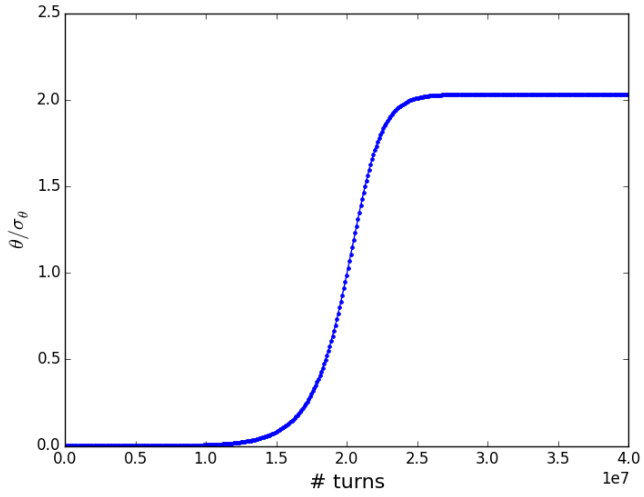

Figure 13: Evolution of the betatron amplitude of an ion in the presence of a circular attractor at $J_0 = 2\sigma_\theta\sqrt{\beta_{CS}}$.

Figure 13 shows a growth of the betatron amplitude of the considered ion. In our simulations it takes the ion $\approx 25 \cdot 10^6$ turns to reach the circular attractor. The period of RHIC revolution is $T = 12.7$ μs. Hence, the expected time of the formation of the phase space doughnut for $\mu/\Delta_t = 2$ is:

$$\tau_{Rt} \approx \frac{(4 \cdot 25 \cdot 10^6[\text{turns}]) \cdot T[\text{sec}]}{60[\text{sec/min}]} \approx 21 \text{ min} \tag{16}$$

During operational cooling the IBS-driven growth time is comparable to the cooling time. Therefore, as was shown in section 3.2, for the ion bunches with design intensity the effect of a circular attractor on bunch dynamics is indistinguishable from the effect of the increased angular spread in electron bunches.

On the other hand, dedicated studies with either reduced intensity of the ions or with comparison of multiple stores with a varied coherent electron-ion angle shall reveal the presence of the attractor in transverse phase space.

For the longitudinal phase space the equivalent of Eq. (15) is:

$$\psi'' + (2\pi)^2\psi = \frac{L_{CS}\gamma F_z(\psi'\sigma_\delta\beta c)}{\sigma_\delta m_i c^2 \beta^2}\text{comb}(0.017) \tag{17}$$

where $\psi \equiv \beta^2 f_s t_l/(\eta\sigma_\delta)$, t_l is a time delay of an ion with respect to the ion bunch center, η is a time slippage over RHIC turn, f_s is a synchrotron frequency, 0.017 is a fraction of synchrotron period in which average ion sees the longitudinal kick from the friction force and we explicitly expressed v_z in $F_z(v_z)$ in terms of ψ'.

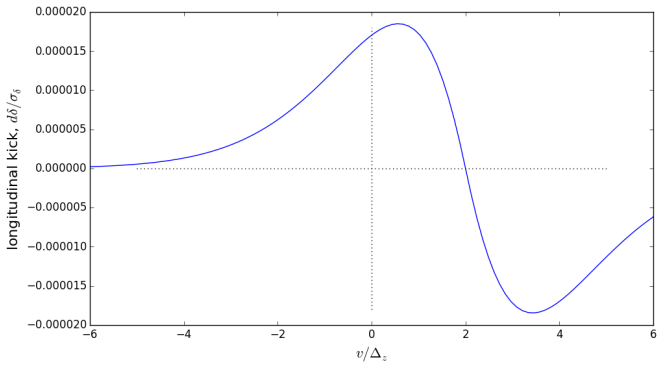

Figure 14: Longitudinal kick for operational LEReC parameters.

To determine the characteristic time of the longitudinal coherent excitation (τ_{Rz}) in LEReC we numerically solve Eq. (17) for an ion with a zero initial synchrotron amplitude. To reduce the simulation's time we assume

that an ion interacts with electron beam on each turn in RHIC. For operational LEReC parameters the longitudinal kick obtained by an ion interacting with the electron bunch on a single pass through the CS is shown in Fig. 14. The force in Fig. 14 is given for coherent offset $\delta = 2\sigma_\delta$.

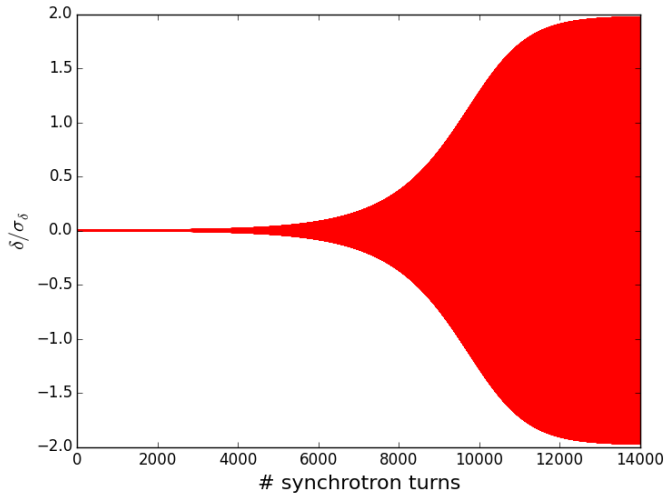

Figure 15: Excitation of an ion with a zero initial synchrotron amplitude in the presence of a circular attractor.

The simulations show (see Fig. 15) that it takes the ion ≈ 14000 synchrotron turns to reach the circular attractor. A period of the synchrotron oscillation for operational RHIC parameters is $T_s = 3.4$ ms. Therefore:

$$\tau_{Rz} \approx \frac{(4 \cdot 14000[\text{turns}]) \cdot T_s[\text{sec}]}{60[\text{sec/min}]} \approx 3 \text{ min} \tag{18}$$

5 Importance of coherent excitation effect for high energy coolers

It was shown above that the coherent excitation effect limits the performance of the cooler. Indeed, if the "large offset conditions" are satisfied, then the ions with small oscillation amplitudes will get excited rather than cooled.

The requirement to the coherent velocity offset is $\mu < \Delta$. Converting it to the beam-alignment requirements in longitudinal ($\mu_\delta = \mu_z/(\beta c)$) and transverse ($\mu_\theta = \mu_{x,y}/(\gamma\beta c)$) phase space one gets:

$$\mu_\delta < \sigma_\delta = \frac{\Delta_z}{\beta c};\ \mu_\theta < \sigma_\theta = \frac{\Delta_t}{\gamma\beta c} \tag{19}$$

For LEReC Eq. (19) sets better than 5×10^{-4} requirement to the alignment of the γ-factors of the electron and ion bunches and better than 140 μrad (at $\gamma = 4.1$) or better than 120 μrad (at $\gamma = 4.9$) requirement to angular alignment of ion and electron trajectories.

For high energy coolers the requirement on γ-matching remains similar to the LEReC requirement. Yet, the requirement to the angular alignment and stability of the trajectories is getting tightened as $1/\gamma$.

For example, for the proposed EIC 275 MeV ring cooler (Table 1) the requirement to angular alignment of the electron and proton trajectories at $\gamma = 293$ is better than 10 μrad.

Table 1: Electron bunch parameters in EIC Ring Cooler.

γ-factor	293.1
geometric $\varepsilon_{x,y}$ [nm]	30, 25
β_{CS} [m]	300
σ_δ	8.6e-4
rms bunch length [cm]	8.9
L_{CS} [m]	170

6 Conclusion

This paper discussed the effect of coherent offset in the velocity distribution of an electron bunch on the beam dynamics of the cooled ions. Under certain conditions such an offset causes coherent excitation of ions with small betatron or synchrotron amplitudes and creates a circular attractor in the ion bunch phase space.

A set of simple formulas describing this effect was derived and applied to simulations of the ion bunch dynamics in LEReC.

It was shown that for the LEReC operational parameters the coherent excitation effect is non-negligible. It was further concluded that the characteristic features of ion beam dynamics in the presence of circular attractor must be observable in LEReC for low intensity ion bunches.

The effect discussed in this paper becomes of special concern to the high-energy cooling due to scaling of angular spread with energy and thus resulting

in a very strict requirement to the relative angular alignment of electron and ion trajectories at high energy.

References

[1] G. I. Budker, An effective method of damping particle oscillations in proton and antiproton storage rings, At. Energ. 22, 346 (1967) [Sov. At. Energy 22, 438 (1967)].

[2] G. I. Budker et al., Experimental study of electron cooling, Part. Accel. 7, 197 (1976).

[3] S. Chandrasekhar, Brownian motion, dynamical friction and stellar dynamics, Rev. Mod. Phys. 21, 3 (1949).

[4] Ya. S. Derbenev and A. N. Skrinsky, The kinetics of electron cooling of beams in heavy particle storage rings, Part. Acc. 8 1 (1977).

[5] D. Caussyn et al., Negative Resistance Instability due to Nonlinear Damping, Phys. Rev. Lett. 73, 2696 (1994).

[6] A. Fedotov et al., Experimental benchmarking of the magnetized friction force, Presentation at COOL05 Workshop (2005).

[7] S. Chandrasekhar, Principles of Stellar Dynamics (Chicago: University of Chicago Press), 1942.

[8] Ya. S. Derbenev and A. N. Skrinsky, The effect of an accompanying magnetic field on electron cooling, Part. Acc. 8 235 (1978).

[9] J. Binney, Dinamical friction in aspherical clusters, Mon. Not. R. astr. Soc. 181, 735-746 (1977).

[10] A. Shemyakin, Formulas for comparing the results of drag force and cooling rates measurements with a non-magnetized cooling model, FERMILAB-TM-2374-AD (2007).

[11] A. Fedotov et al., Physics guide of BETACOOL code Version 1.1, BNL Technical Note C-A/AP/262 (2006).

[12] R. D. Ruth, IEEE Trans. Nucl. Sci., NS-30, 2669 (1983).